minerals

MDPI

Article

Direct Adherence of Fe(III) Particles onto Sheaths of *Leptothrix* sp. Strain OUMS1 in Culture

Tatsuki Kunoh [1,2], Hideki Hashimoto [1,3], Tomoko Suzuki [1,4], Naoyuki Hayashi [1,2,5], Katsunori Tamura [1,2], Mikio Takano [1,2], Hitoshi Kunoh [1,2] and Jun Takada [1,2,*]

Received: 15 November 2015; Accepted: 11 January 2016; Published: 18 January 2016
Academic Editor: Karen Hudson-Edwards

1 Core Research for Evolutionary Science and Technology (CREST), Japan Science and Technology Agency (JST), Okayama 700-8530, Japan; tkunoh06@cc.okayama-u.ac.jp (T.K.); hideki-h@cc.kogakuin.ac.jp (H.H.); suzukit@fc.jwu.ac.jp (T.S.); hayashi@icems.kyoto-u.ac.jp (N.H.); ktamura@cc.okayama-u.ac.jp (K.T.); takano@cc.okayama-u.ac.jp (M.T.); hkunoh@cc.okayama-u.ac.jp (H.K.)
2 Graduate School of Natural Science and Technology, Okayama University, Okayama 700-8530, Japan
3 Department of Applied Chemistry, School of Advanced Engineering, Kogakuin University, Hachiohji, Tokyo 192-0015, Japan
4 Department of Chemical and Biological Science, Japan Woman's University, Bunkyo-ku, Tokyo 112-8681, Japan
5 Institute of Integrated Cell-Material Sciences, Kyoto University, Kyoto 606-8317, Japan
* Correspondence: jtakada@cc.okayama-u.ac.jp; Tel./Fax: +81-86-251-8106

Abstract: *Leptothrix* species, one of the Fe/Mn-oxidizing bacteria, oxidize Fe(II) and produce extracellular, microtubuar, Fe-encrusted sheaths. Since protein(s) involved in Fe(II) oxidation is excreted from *Leptothrix* cells, the oxidation from Fe(II) to Fe(III) and subsequent Fe(III) deposition to sheaths have been thought to occur in the vicinity or within the sheaths. Previously, Fe(III) particles generated in MSVP medium amended with Fe(II) salts by abiotic oxidation were directly recruited onto cell-encasing and/or -free sheaths of *L. cholodnii* SP-6. In this study, whether this direct Fe(III) adherence to sheaths also occurs in silicon-glucose-peptone (SGP) medium amended with Fe(0) (SGP + Fe) was investigated using another strain of *Leptothrix* sp., OUMS1. Preparation of SGP + Fe with Fe powder caused turbidity within a few hours due to abiotic generation of Fe(III) particles via Fe(II), and the medium remained turbid until day 8. When OUMS1 was added to SGP + Fe, the turbidity of the medium cleared within 35 h as Fe(III) particles adhered to sheaths. When primitive sheaths, cell-killed, cell-free, or lysozyme/EDTA/SDS- and proteinase K-treated sheath remnants were mixed with Fe(III) particles, the particles immediately adhered to each. Thus, vital activity of cells was not required for the direct Fe(III) particle deposition onto sheaths regardless of *Leptothrix* strains.

Keywords: *Leptothrix*; strain OUMS1; abiotic oxidation of Fe(0) to Fe(III); Fe encrustation of sheaths; direct deposition of Fe(III) onto sheaths

1. Introduction

In nature, organisms frequently produce unique, ingenious structures with specific benefits (e.g., to protect themselves, to stock and utilize nutrients, to move and work smoothly) by biomineralization [1]. Species of the genus *Leptothrix*, an Fe/Mn-oxidizing bacterium, inhabit aqueous environments such as freshwater Fe/Mn-rich seeps and wetlands where groundwater outwells [2,3]. They form filamentous-looking microtubular, cell-encasing sheaths when copious amounts of oxidized Fe or Mn precipitate from the water or solution [2,3]. Extracellular polymers from microbial cells in general are believed to facilitate microbe–colloid attachment and aggregation of biogenic particles on cell surfaces

when biofilms are formed in aquatic environments [4,5]. Actively dividing *Leptothrix* cells also excrete exopolymers from their surface, which seemingly provide a platform for the metal-, in particular, Fe-enriched sheaths [6,7].

An electron is generated during biogenic oxidation of aqueous-phase Fe(II) to Fe(III) or Mn(II) to Mn(IV) and has long been thought to be essential for autotrophic or mixotrophic metabolism in *Leptothrix* as an energy source [4,8–13]. The Fe/Mn-oxidizing proteins of *L. discophora* SS-1 (hereafter referred to as SS-1) were reported to be excreted from bacterial cells in association with exopolymers [8,14–16]. A 108-kDa Mn-oxidizing protein and a ~150-kDa Fe-oxidizing protein were identified in concentrated spent cultures of *L. cholodnii* SP-6 (hereafter referred to as SP-6) [17] and of SS-1 [8], respectively. These metal-oxidizing proteins (corresponding to enzymes) are considered to contribute to oxidation of Fe(II)/Mn(II) and be associated with formation of the *Leptothrix* sheath and its metal encrustation [8,9,14,15,17].

The metal encrustation of *Leptothrix* sheaths is considered to result from the interaction between active groups on the bacterial organic components that comprise the sheath skeleton and aqueous-phase inorganics [4]. Indeed, the sheath material of *Leptothrix* contains organics such as polysaccharides, proteins, and lipids whose active groups are expected to play critical roles to bind aqueous-phase cations [3,6,18,19]. Chan *et al.* [4] showed a strong correlation between the presence of acidic polysaccharides with carboxyl functional groups to the distribution of iron oxyhydroxides in *Leptothrix* sheath and *Gallionella* stalks. The nearly uniform distribution of inorganics over the entire *Leptothrix* sheaths, harvested from natural environments [20] or a relatively long-term (7–14 days) culture [17,21], suggests that the active groups on the organic components that comprise the core skeleton of sheaths are involved in binding aqueous-phase inorganics. All these data suggest that negatively charged active groups of saccharic and proteinaceous acidic components in sheath organics of bacterial origin aid in attracting aqueous-phase metal ions [4,5].

In light of these earlier data, encrustation of inorganics in sheaths is most likely the result of biotic metaloxidization, and any associated reactions are presumably concerned with energy metabolism in *Leptothrix* cells [22]. Although careful approaches to study the interactions between bacterial exopolymers and metal ions in aqua-environments have promoted our understanding of this matter, how metal-oxidizing factors, for either Fe or Mn, are structurally associated with complex organic/inorganic composites such as *Leptothrix* sheaths still remains to be elucidated in more detail.

Irrelevant to any biotic metaloxidization theory, we recently provided microscopic and spectroscopic evidence that the deposition of Fe(III) precipitates that are generated by abiotic oxidation directly onto sheaths of SP-6 cells in culture media amended with Fe(II) salts is actually independent of vital activity of bacterial cells [23]. Although it is still unclear how this direct adherence opposes the hypothesized modes of sheath encrustation, we must consider the direct nature of this deposition when investigating the interactions between bacterial exopolymers and metal ions, particularly in shake cultures and whether this direct deposition is unique to the SP-6 strain of *Leptothrix*.

To date, a variety of industrial functions such as lithium-ion battery anode material [24,25], catalyst enhancer [26–28], and porcelain pigment [29] have been discovered for the sheaths of *Leptothrix*. Our previous study further indicated that the chemical character and crystallinity of the sheath matrix can be modified depending on the culture conditions for the strains, especially on the components of the medium [30]. These findings encouraged us to elucidate the encrustation mechanism of sheaths in culture in more detail so that we can rationally manipulate the matrix and elemental composition of *Leptothrix* sheaths to further increase the usefulness of the material and to create novel functional materials.

In this study, we demonstrate that the direct adherence of abiotically formed Fe complexes onto sheaths also occurs in *Leptothrix* sp. strain OUMS1 in an Fe(0)-containing culture medium and that the presence of bacterial cells is not essential for this direct adherence of Fe complexes.

2. Experimental Section

2.1. Strains, Medium and Culturing

Leptothrix sp. strain OUMS1 (NITE BP-860) (hereafter referred to as OUMS1) isolated from flocculent, ocherous deposits in a biological freshwater purification plant in Joyo City, Kyoto Prefecture, Japan [21] was used in this study. Cells recovered from a frozen stock culture were streaked on silicon-glucose-peptone (SGP) agar [21] and incubated at 20 °C for seven days. Single colonies were transferred to 25 mL of SGP broth in 50 mL conical tubes and incubated on a rotary shaker (EYELA FMC-1000, Tokyo Rikakikai, Tokyo, Japan) at 20 °C and 70 rpm. After two to three days, 1–5 mL of the cell suspension (adjusted to 10 cfu/mL by densitometry (Nanodrop 2000C, Thermo Fisher Scientific, Waltham, MA, USA)) was transferred to 100–500 mL of SGP or SGP broth containing 14 g/L Fe(0) powder (~150 μm diameter) (Wako Pure Chemical, Osaka, Japan) (hereafter referred to as SGP + Fe) in glass flasks [31], then incubated for 2–14 days.

2.2. Streptomycin Treatment to Kill Cells within Sheaths

Exponentially growing cells cultured in 100 mL of SGP broth for two days were harvested, resuspended in 500 μL of 0–100 mg/mL aqueous streptomycin solution (Nacalai Tesque, Kyoto, Japan), and incubated for 30 min at room temperature. Cells were then washed twice in sterile ultrapure water (UPW) (5 min each) to wash out the streptomycin, and the resultant cell suspension was dropped onto SGP agar plates, then incubated for four to five days at 20 °C (drop test) to examine the lethality of the streptomycin. Since 0.1 mg/mL streptomycin was sufficient to kill all the cells, this concentration was used in the 30-min step to kill the exponentially growing cells. To examine whether abiotically formed Fe particles are deposited onto the sheaths encasing dead cells, we washed the streptomycin-treated sheaths five times in SGP broth, added them to SGP + Fe, and incubated them at 20 °C and 70 rpm for two weeks.

2.3. Differential Interference Contrast Microscopic Observation after Adherence of Fe Particles on Sheath Surfaces

Cells were cultured in 25 mL of SGP broth for two days. SGP + Fe alone was separately incubated for two days to generate abiotic Fe particles (Fe particle-suspending medium). An equal volume of the cell culture suspension and the Fe particle-suspending medium were mixed in a 1.5 mL Eppendorf tube and immediately examined with differential interference contrast optics and a light microscope (hereafter DIC) (BX51 system microscope, Olympus, Tokyo, Japan) to check for adherence of Fe(III) particles on sheath surfaces.

2.4. Lysozyme-EDTA-SDS (LES)-Proteinase K Treatment of the Sheaths

According to the procedure described previously [19], exponentially growing cells were harvested by centrifugation at 3600× *g* for 10 min. The cell pellet was washed with UPW twice (5 min each), suspended in 20 mL of the lysis solution consisting of 2.5 mM ethylenediaminetetraacetic acid (EDTA) (Nacalai Tesque) and 150 μg/mL of lysozyme (Sigma-Aldrich, St. Louis, MO, USA), and incubated at 37 °C for 1 h. Then sodium dodecyl sulfate (SDS) was added to the reaction mixture at a final concentration of 1%. The mixture was incubated on a shaking mixer (LMS, Tokyo, Japan) at room temperature for 12 h to disrupt the cells. The cell remnants were repeatedly (five times) washed out of the sheath samples with UPW (hereafter referred to as Lysozyme-EDTA-SDS (LES) treatment). For the subsequent proteinase K treatment, the washed sheaths were resuspended in 20 mL of Tris/EDTA (TE) buffer (pH 8.0) containing 0.6% SDS and 50–100 μg/mL proteinase K (Nacalai Tesque) and incubated at 37 °C for 1.5 h, then washed with UPW as before to obtain sheath remnants (hereafter referred to as ProK treatment). Removal of cells from sheath remnants was checked using phase contrast optics and the light microscope (hereafter PCM).

2.5. SDS-PAGE (Polyacrylamide Gel Electrophoresis) and Silver Staining to Confirm Removal of Protein from Sheath Remnants

The LES- or LES/ProK-treated sheath samples were separated electrophoretically using 10% SDS-PAGE. The gels were stained using a SilverQuest Silver Staining Kit (Life Technologies, Carlsbad, CA, USA). For reference, the untreated cell-encasing sheath sample was also loaded on the gel.

2.6. Scanning Electron Microscopy (SEM) and Energy-Dispersive X-Ray Spectroscopy (EDX)

The sheath samples (cultured-, streptomycin-, LES-, or LES/ProK-treated sheaths) were fixed with 2.5% glutaraldehyde (Electron Microscopy Sciences, Hatfield, PA, USA) in 0.1 M cacodylate buffer (pH 7.0) at 4 °C overnight. They were further fixed with 1% OsO_4 in the same buffer for 15 min, followed by washing with UPW three times. Then they were dehydrated in an ethanol series (30%, 50%, 70%, 95% and 100%) and 100% *t*-butanol (10 min each) at each concentration; at each step, the samples were collected by a 5-min centrifugation at 2400× *g*. After the final solvent exchange, the samples were freeze-dried and transferred to carbon tape on an Scanning Electron Microscopy (SEM) copper stub.

For reference, Fe particles formed in SGP + Fe were analyzed by SEM/EDX (Energy-Dispersive *X*-Ray Spectroscopy). The Fe powder was added to SGP broth (1.4 mg/mL) and incubated on a rotary shaker at 70 rpm for 25 h. The resultant Fe particles were harvested by centrifugation at 14,000× *g* for 5 min, then washed with 100% ethanol. The ethanol suspension was dropped onto carbon tape on an SEM stub and air-dried before SEM observation.

When necessary, the specimens were coated with platinum before observation with an SEM equipped with EDX (S-4300, Hitachi, Tokyo, Japan) operated at an accelerating voltage of 15 kV. Atomic percentages of major inorganics detectable in sheaths were measured by EDX and expressed as the mean with standard deviation (hereafter referred to as s.d.) for at least 10 spot values.

2.7. Transmission Electron Microscopy (TEM), High-Angle Annular Dark Field-Scanning Transmission Electron Microscopy (HAADF-STEM) and Energy Dispersive X-Ray Spectroscopy (EDX)

Samples were prepared as described previously [6]. Briefly, the sheath samples were collected by centrifugation and fixed with a mixture of 2.5% glutaraldehyde, 1% OsO_4, and 4.5% sucrose in 0.1 M cacodylate buffer (pH 7.0) on ice for 2 h and then embedded in 3% agar. Small pieces of the agar block were dehydrated through a graded series of ethanol for final embedment in Quetol 651 resin (Nisshin EM, Tokyo, Japan). Ultrathin sections were stained with uranyl acetate and lead solutions and transferred to copper grids. For the EDX mapping analysis, a formvar film on the grid and carbon coating of samples were required. The sections were observed with a Transmission Electron Microscopy (TEM) (H-7500, Hitachi, Tokyo, Japan) or HAADF-STEM (JEOL JEM-2100F TEM equipped with CEOS Cs corrector (for spherical correction)) and an EDX detector (JEOL JED-2300T, Tokyo, Japan).

2.8. Determination of Fe(II) and Fe(II) + Fe(III) Concentrations in Culture Medium with O-Phenanthroline

Concentration changes of Fe(II) and Fe(II) + Fe(III) in SGP + Fe over time during the incubation were determined using a published method [32] with modifications. To determine Fe(II) concentrations, 0.5 mL of the medium was centrifuged at 1500× *g* for 5 min, then 0.5 mL of the resultant supernatant was added to 0.25 mL of acetic acid buffer (pH 4.6) and 5 mM *O*-phenanthroline, and the solution was brought to 5 mL with UPW. After gentle agitation, the reaction mixture stood at room temperature for 30 min to yield the reddish orange Fe(II)-chelate with *O*-phenanthroline, followed by determination of absorbance (OD) at 510 nm with NanoDrop 2000C (Thermo Fisher Scientific). The background absorbance at 700 nm was subtracted from the measured value at 510 nm.

For Fe(II) + Fe(III) concentrations, 0.5 mL of 3 N HCl was added to 0.125–0.25 mL of sampled medium and brought to 3 mL with UPW. The mixture was then heated in boiling water for 5 min and filtered through 0.2 μm filter (Sartorius Stedim Biotech, Goettingen, Germany). To reduce acid-soluble

Fe(III), 0.1 mL of 1.44 M HCl-hydroxyamine was added to the resultant mixture, followed by 0.25 mL of 5 mM *O*-phenanthroline. After the pH was adjusted to 3.5 with 6 N aqua ammonia, 0.25 mL of acetic acid buffer (pH 4.6) was added to the reaction mixture. The total volume was then brought to 5 mL with UPW, and after 30 min, the optical density (OD) at 510 nm was measured. Theoretically, the acid and hydroxylamine treatments should reduce Fe(III) to Fe(II), which has a maximal OD at 510 nm. Thus, the Fe(II) + Fe(III) concentration is technically equivalent to the concentration of acid-soluble Fe in the medium. Note that Fe(III)-chelate with *O*-phenanthroline does not absorb 510 nm wavelengths. Fe concentrations were then estimated using a standard curve based on serial dilutions of 1 g/L ammonium Fe(II) sulfate in 0.012 N HCl.

2.9. Mössbauer Analysis of Precipitated Fe Particles Formed in Medium

Precipitates formed in the media for 25 h were harvested by centrifugation and freeze-dried. For ^{57}Fe Mössbauer spectroscopy, transmission geometry was used with ^{57}Co/Rh as the radiation source, and a-Fe as a control for velocity calibration and center shift [33]. The collected spectra were computer-fitted using the Lorenzian function [33].

3. Results and Discussion

3.1. Generation of Fe(III) Particles Containing P and Si in SGP + Fe by Abiotic Oxidation

Suzuki *et al*. [31] reported that yellowish brown sheaths with attached Fe particles formed when OUMS1 cells were cultured in SGP + Fe, while those cultured in SGP lacking an Fe source remained whitish, suggesting that in SGP + Fe, metal iron, Fe(0), could be oxidized to Fe(III), which was deposited onto the sheaths. In this study, the uninoculated SGP + Fe medium looked clear immediately after preparation but became turbid within 5 h (Figure 1A). The color of the turbidity gradually changed from lightly to deeply yellowish within 15 h (Figure 1A). The colorimetric iron determination using *O*-phenanthroline revealed that the Fe(II) concentration in SGP + Fe peaked by 5 h, began to decline by 15 h, and by 25 h was less than 40 μM (Figure 1B), while the Fe(II) + Fe(III) concentration in the medium increased until 15 h and remained nearly constant thereafter (Figure 1C). Because abiotic Fe oxidation Fe(II) to Fe(III) in fully oxygenated water at circumneutral pH is very rapid (half-life < 1 min) [22,34], reduction of Fe(II) concentration might result in discontinued Fe(III) generation. We reported that MSVP medium [35] with high Fe(II) concentrations became visually turbid due to Fe(III) precipitation within 20 min after addition of Fe(II) salts [23]. On the basis of the onset of turbidity, Fe(III) precipitation was much more delayed in SGP + Fe than in MSVP. This delay probably reflects a slow release of Fe(II) from Fe(0) in the medium with Fe powders (Figure 1B).

When the precipitates responsible for the medium turbidity were harvested and observed with SEM. The precipitates in SGP + Fe collected at 25 h were composed of aggregated globular particles nearly 50 nm diameter (Figure 1D). In the subsequent EDX analysis, Fe, P and Si were the major inorganics in the particles, and Na, Mg, S, and Ca were the minor (Figure 1E). The Mössbauer analysis indicated that these precipitates comprised 100% Fe(III) (Figure 1F). These findings indicate that Fe(0) was abiotically oxidized to Fe(III) via Fe(II) and resulted in the formation of globular particles containing Fe(III), P, and Si as major inorganics in SGP + Fe.

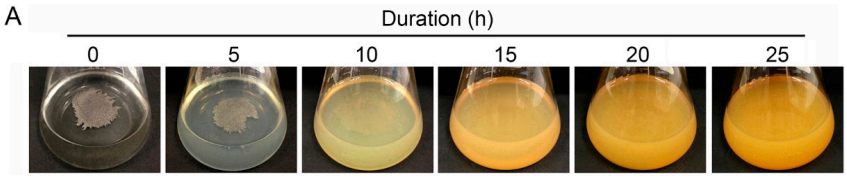

Figure 1. *Cont*.

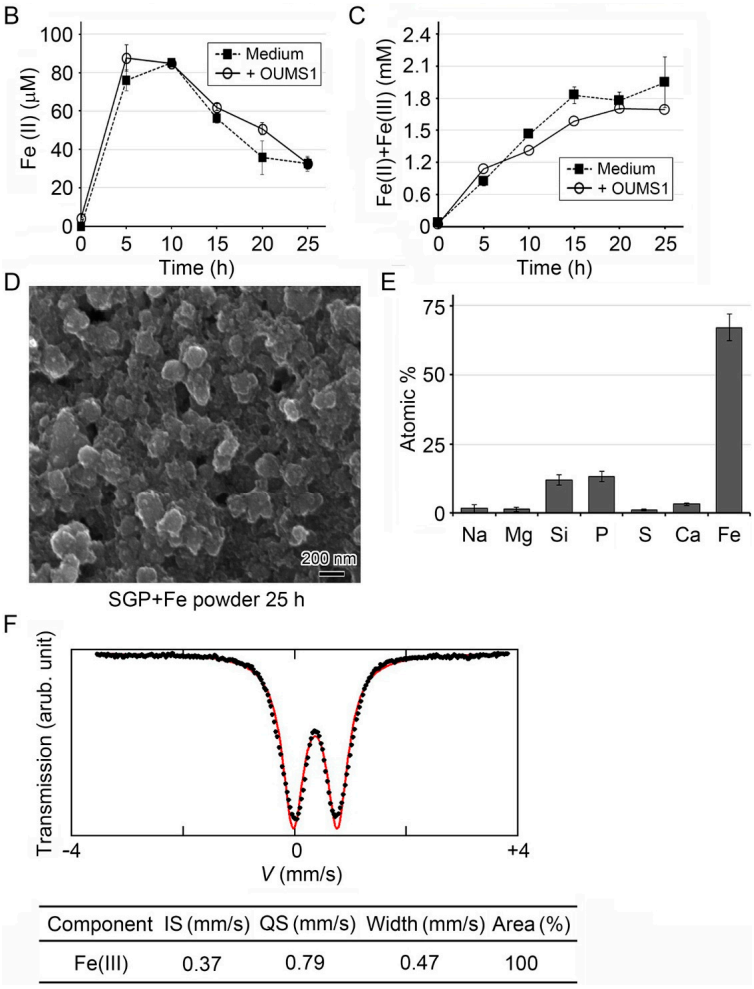

Component	IS (mm/s)	QS (mm/s)	Width (mm/s)	Area (%)
Fe(III)	0.37	0.79	0.47	100

Figure 1. Fe(III) particles generated abiotically in uninoculaated SGP + Fe medium. (**A**) Visual changes in medium turbidity in uninoculated SGP + Fe; (**B**,**C**) Time course of change in mean (± s.d.) concentrations of Fe(II) (**B**) and Fe(II) + Fe(III) (**C**) in uninoculated (closed square) or inoculated (open circle) SGP + Fe. At least three replicates were used for each treatment; (**D**) SEM image of the particles harvested from SGP + Fe after 25 h incubation; (**E**) Atomic percentages of detectable major inorganics in the particles harvested from SGP + Fe after 25 h incubation (determined by EDX). Expressed as mean ± s.d. from $n = 10$ spots per sample; (**F**) Mössbauer spectrum of Fe particles generated in SGP + Fe after 25 h incubation. Note that the Fe component consisted of 100% Fe(III).

3.2. Adherence of Fe(III) Particles Preformed in SGP + Fe to Sheath Surfaces of OUMS1

Uninoculated SGP + Fe remained turbid until day 8 after the medium was prepared (Figure 2A), suggesting that the generated Fe(III) particles were stable in the medium. In contrast, the inoculated SGP + Fe had gradually turned clear by 10 h as the cells multiplied and remained clear (Figure 2A); the brownish colony clusters on the bottom and side wall of the flasks are considered to be colored by deposits of the turbid material (plausibly Fe-hydroxides and/or -oxyhydroxides formed by abiotic oxidation [22]) onto the sheaths. Vollrath and colleagues [36,37] reported that the rate of microbial Fe(II) oxidation by *L. cholodnii* Appels is significantly faster than that of abiotic oxidation. However, in the present study, the change in Fe(II) and/or Fe(II) + Fe(III) concentrations in the inoculated SGP + Fe over time were quite similar to that in the respective uninoculated medium (Figure 1B,C), suggesting that abiotic oxidation of Fe(0) to Fe(III) via Fe(II) proceeded similarly regardless of the presence or absence of OUMS1.

Light microscopy confirmed that the aggregated precipitates adhered to the sheath surfaces in SGP + Fe. Subsequent SEM (Figure 2B) and EDX (Figure 2C) showed that the precipitates were composed of nano-scaled particles that had a globular shape and contained inorganic components similar to those formed in the uninoculated medium (Figure 1D,E). The Mössbauer analysis also revealed that these particles comprised ~99% Fe(III) and ~1% Fe(0) (Figure 2D). The detected Fe(0) is probably a contaminant from the Fe(0) powder originally used for medium preparation, although a magnet was used to remove as much powder as possible from the medium. These results strongly suggest that the Fe(III) particles that formed abiotically in the medium attached directly onto the sheath surfaces.

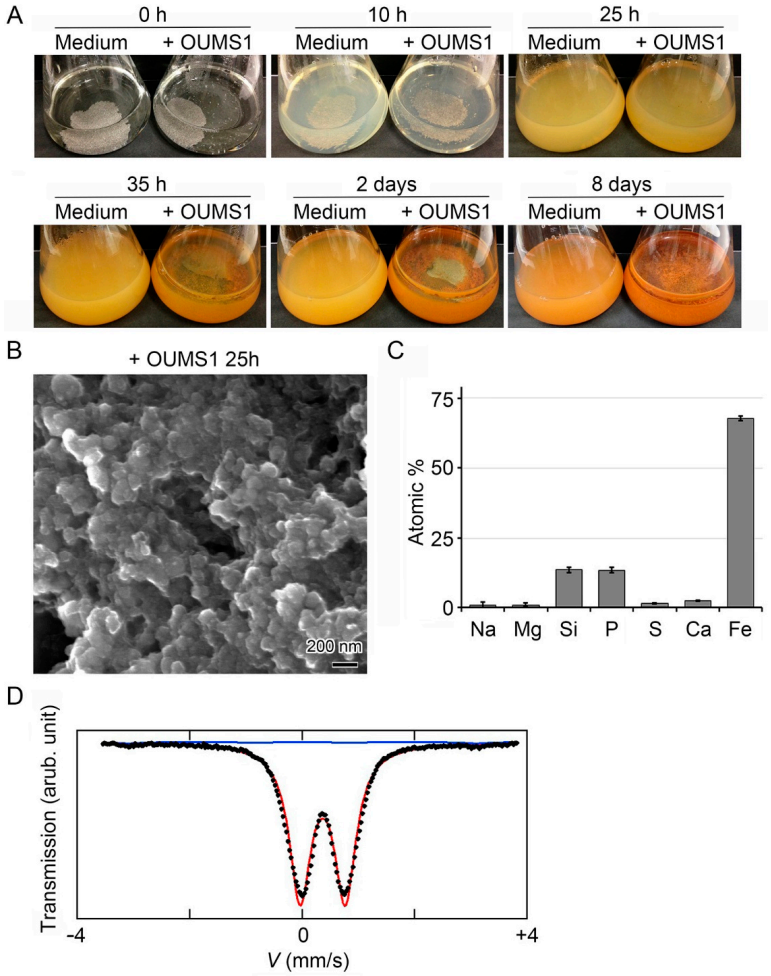

Component	IS (mm/s)	QS (mm/s)	Width (mm/s)	Area (%)
Fe(III)	0.37	0.80	0.47	98.9
Fe(0)	0.00	0.00	0.43	1.1

Figure 2. Adherence of Fe(III) particles abiotically generated in SGP + Fe medium to OUMS1 primitive sheaths. (**A**) Visual changes in medium turbidity in uninoculated (**left**) or inoculated (**right**) SGP + Fe; (**B**) SEM image of the particles harvested with OUMS1 from SGP + Fe after 25 h incubation; (**C**) Mean (± s.d.) atomic percentages of detectable major inorganics in the particles harvested with OUMS1 from SGP + Fe after 25 h incubation (determined by EDX). n = 10 spots per sample; (**D**) Mössbauer spectra of Fe particles harvested with OUMS1 from SGP + Fe after 25 h incubation. Note that the Fe component consisted of nearly 99% Fe(III) and 1% Fe(0) probably derived from the iron powder added to the medium.

These observations also suggest that clearance of the turbidity as the cells multiplied in the inoculated SGP + Fe might reflect the progressive adherence of the preformed Fe(III) particles onto the sheath surfaces. To test this possibility, whitish primitive sheaths preformed in SGP (Figure 3A, left) were mixed with a suspension of Fe(III) particles that had been separately generated in uninoculated SGP + Fe (Figure 3A, center). Within a few minutes, the primitive sheath clusters turned brownish (Figure 3A, right). DIC micrographs (Figure 3B–D) demonstrate the stepwise binding process of abiotically oxidized Fe(III) particles to the primitive sheaths. Analysis with SEM/EDX also showed a strong Fe signal from these attached particles (data not shown). Again, these results confirmed that Fe(III) particles preformed in the medium adhered directly to the sheath surface.

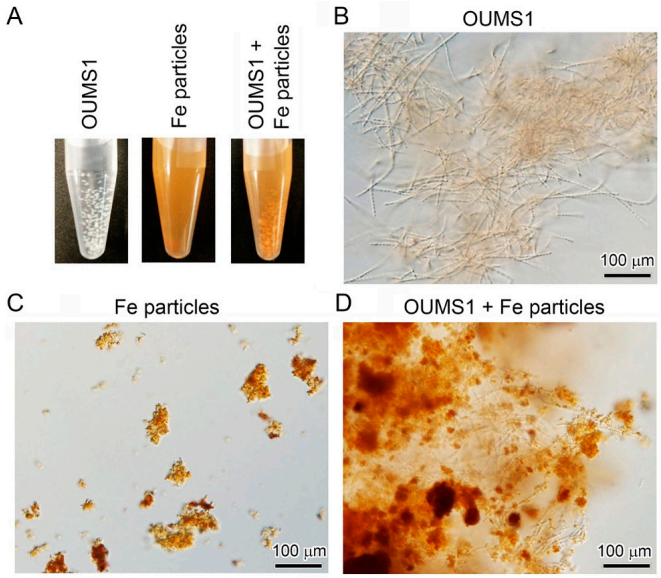

Figure 3. Fe(III) particles adhered onto sheaths of OUMS1 cultured in Fe-free medium. (**A**) Whitish primitive sheaths formed in Fe-free SGP (**left**) and abiotically generated Fe(III) particles in SGP + Fe (**middle**). Mixture of both in a tube (**right**). Note that the whitish sheaths immediately turned brownish after mixing with Fe(III) particles; (**B**) DIC images of cells and associated sheaths cultured in Fe-free medium; (**C**) Abiotically generated Fe(III) particles; (**D**) The particle assembly adhered to sheaths after mixing (**B**) with (**C**).

3.3. Encrustation of "Cell-Killed" and "Cell-Free" Sheaths of OUMS1 with Numerous Fe(III) Particles after Incubation in SGP + Fe

TEM observations revealed that OUMS1 cells of a one-day-old culture were encompassed by a thin primitive sheath across an intervening space in SGP (Figure 4A, left), whereas a number of electron-dense particles (probably Fe(III) complexes generated in the medium) adhered to the hairy sheath of OUMS1 cultured in SGP + Fe by day 3 (Figure 4A, right). To examine whether bacterial cells encased with sheaths were involved in the direct deposition of Fe(III) onto the sheaths, "cell-killed" or "cell-free" sheaths were prepared and then treated with SGP + Fe. Before the treatment, the lethal effects of streptomycin on cells encased with sheaths were confirmed by a drop test. The bacterial cells multiplied in the control (no streptomycin treatment), but colonies never developed after any streptomycin treatments (Figure 4B), indicating that streptomycin definitely killed the cells encased with sheaths. SEM images showed that the untreated cells were enveloped by sheaths with smooth surfaces (Figure 4C, left), while the surfaces of sheaths enveloping the treated cells looked wrinkled, probably from a loss of turgor caused by cell death within the sheaths (Figure 4C, right). After the treated sheaths were incubated in SGP + Fe for two weeks, TEM illustrated that the streptomycin-treated cells degenerated, resulting in distorted plasma membranes and loss of cytoplasm (Figure 4D, left) and that a number of electron-dense particles corresponding to Fe(III)

adhered to the sheath remnants (Figure 4D, right). Thus, cell activity is not required in deposition of Fe(III) particles onto the sheaths.

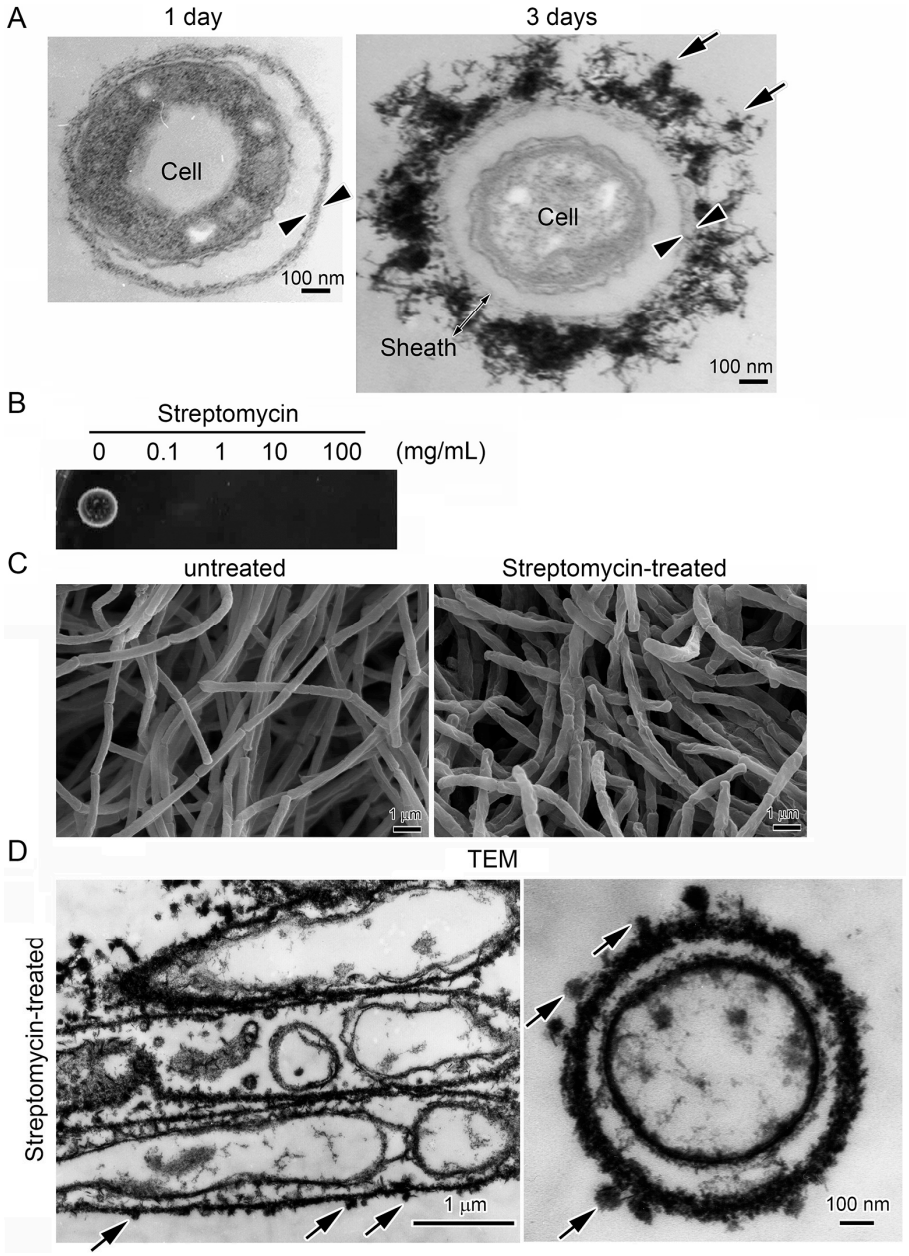

Figure 4. Adherence of electron-dense particles onto sheath remnants of streptomycin-killed cells (**A**) TEM images of sheaths after 1 day (**left**) and 3 days (**right**) of incubation in SGP + Fe. Arrowheads: thin primitive sheaths, arrows: electron-dense particles. Note that electron-dense particles only adhered to the loosely woven projections outside the thin primitive sheath (**right**); (**B**) Cells were sensitive to ⩾0.1 mg/mL streptomycin (SM), as determined by a spot test on SGP agar; (**C**) SEM images of SM-treated sheaths (**right**) and untreated sheaths (**left**); (**D**) TEM images of SM-treated sheaths after 14 days incubation in SGP + Fe. Note the degenerated cytoplasm enveloped by distorted plasma membrane. Arrows indicate electron-dense particles that correspond to Fe(III) abiotically generated in the medium.

Subsequently, the possibility that Fe(III) particles were deposited onto "cell-free" sheaths was examined using lysozyme-SDS-EDTA (LES)-treated sheaths. Before the LES treatment, the presence of cells within smooth-surfaced sheaths was confirmed by PCM and SEM (Figure 5A, upper). After the

LES treatment, the sheaths became empty (Figure 5A, lower left), and the remnant sheaths changed into a sheet-like structure after freeze-drying (Figure 5A, lower center). A high magnification SEM illustrates that the texture of the sheet-like structure was composed of woven nano-scaled fibers, which were exposed at the sheet surfaces (Figure 5A, lower right). Subsequent treatment of the LES-treated sheaths with SGP + Fe caused adherence of Fe(III) particles around the sheath remnants (Figure 5B), evidently indicating that Fe(III) was deposited onto "cell-free" sheaths.

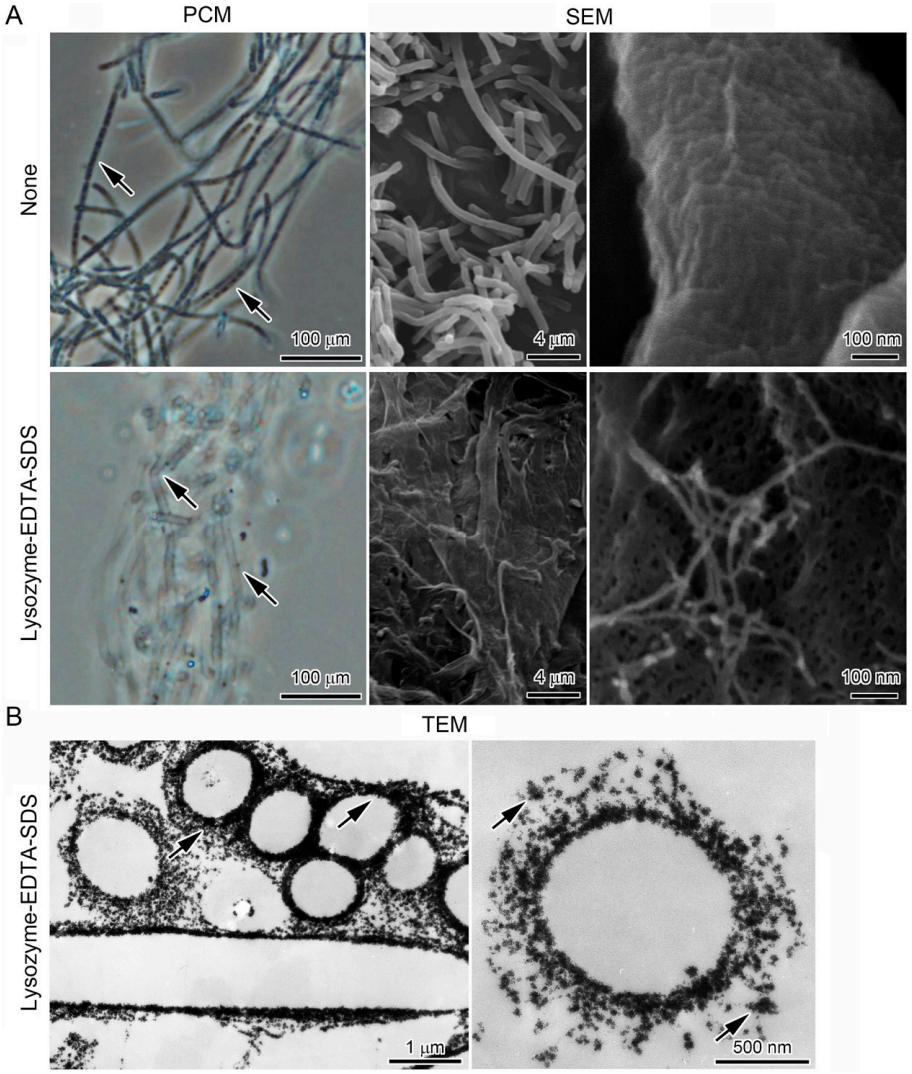

Figure 5. Adherence of electron-dense particles onto LES-treated sheath remnants. (**A**) PCM and SEM images of LES-treated sheaths (**lower**) and untreated sheaths (**upper**). Note that the treatment successfully released nano-scaled fibrils from sheaths (**lower right**); (**B**) TEM images of LES-treated sheaths after 14 days incubation in SGP + Fe. Note that the treatment successfully removed cells, leaving the sheath remnants. Arrows indicate electron-dense particles that correspond to Fe(III) abiotically generated in the medium.

3.4. Deposition of Fe Particles onto the LES- and Proteinase K-Treatments

As described already, some isolates of *Leptothrix* excrete Mn-oxidizing enzyme(s) [8,17], and the enzyme activity was retained in lysozyme/EDTA/*N*-lauryl sarcosine-treated sheaths [17]. To examine whether these oxidizing enzymes are involved in deposition of Fe(III) particles onto sheaths, the LES-treated sheaths were further deproteinized by proteinase K (hereafter, ProK-treatment), then incubated for two weeks in SGP + Fe. SDS-PAGE/silver staining revealed that almost all

proteins less than 200 kDa in the untreated cell-encasing sheaths and in the LES-treated sheaths were completely lysed by the ProK-treatment; a nearly immobile fraction with a high molecular weight (greater than ~250 kDa) was also detected (Figure 6A). This fraction presumably corresponds to glycoproteins [18,19,38] or to highly chemically/enzymatically resistant active protein clusters that have Fe-oxidizing activity.

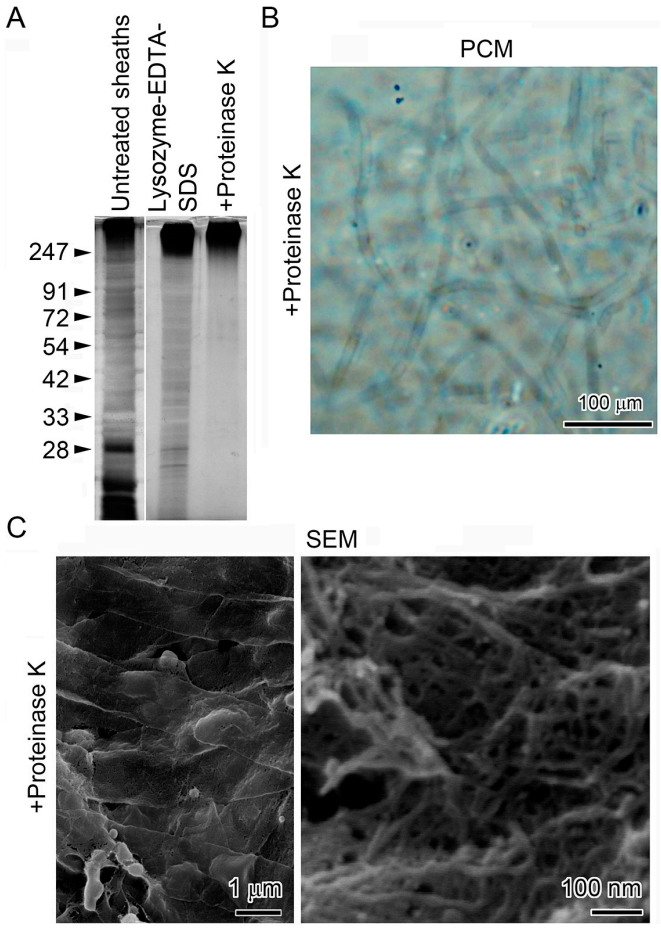

Figure 6. Structural alteration of tubular structures and fine fibrils of LES-treated sheaths after ProK treatment. (**A**) Silver-stained SDS-PAGE gel loaded with the untreated cell-encasing sheath fraction (**left lane**) and with those treated with LES (**middle lane**) or LES/ProtK (**right lane**). Note the high molecular weight material (>250 kDa, probably corresponding to glycoprotein) that did not migrate at the top of each lane; (**B**) PCM image of sheath remnants after ProK treatment; (**C**) SEM images of LES/ProK-treated sheaths. Note nano-scaled fibrils released from sheaths (**right**).

PCM and SEM images confirmed that the ProK-treatment did not prominently alter the tubular structure and fine fibrils of the LES-treated sheaths (Figure 6B,C). In high-angle annular dark field-scanning transmission electron microscopy (HAADF-STEM) images, numerous precipitates adhered to the ProK-treated and cell-free sheaths after the two-week incubation (Figure 7A). Furthermore, EDX detected Fe in these precipitates (Figure 7B) and an extremely high atomic percentage of Fe in the sheaths harboring these particles (Figure 7C). On the basis of the present results, we concluded that proteins less than 200 kDa in sheath fibrils were not required for the direct deposition of Fe particles onto sheaths.

Both Fe- and Mn-oxidizing factors of SS-1 with a molecular weight of 150 kDa were detected in the medium and/or the cell lysate [8]. Similarly, a Mn-oxidizing factor with a molecular weight of 108 kDa was detected in the spent culture medium, distilled-water-washed cells and

sheaths, and cell-free sheaths of *Leptothrix cholodnii* SP-6 [17]. These earlier reports led us to hypothesize that Fe/Mn-oxidizing enzymes of OUMS1, if any, might have a similar molecular weight (<200 kDa) and thus could be lysed by the ProK treatment. However, the possibility should not be ruled out that a fraction with a molecular weight higher than ~250 kDa (Figure 6A) may be highly chemically/enzymatically resistant active protein clusters associated with Fe-oxidizing factors and may be involved in Fe oxidation. We still need to test whether the direct deposition of Fe particles is related to the activity of Fe/Mn-oxidizing enzymes.

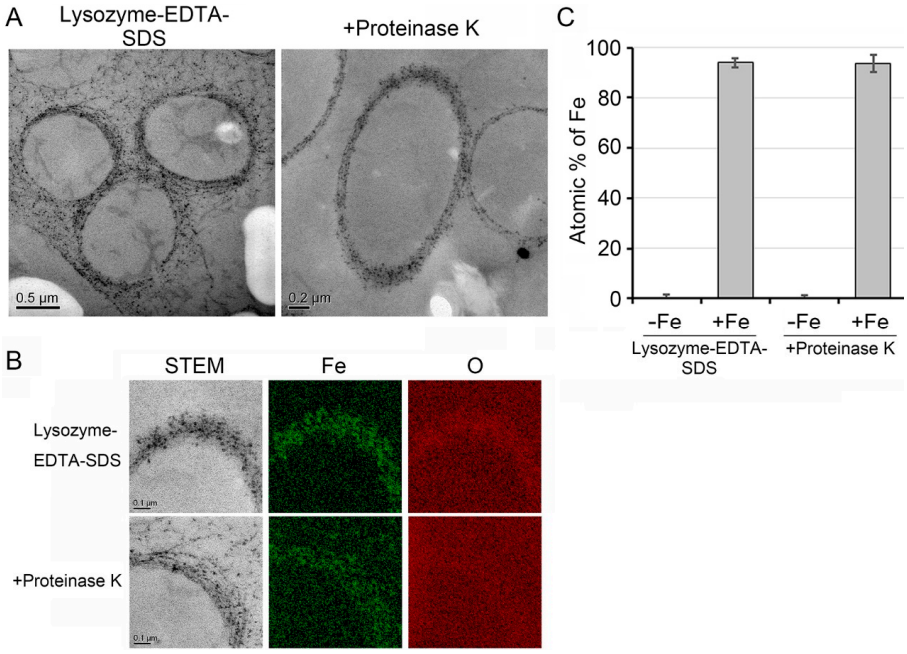

Figure 7. Adherence of Fe particles onto both LES- and LES/ProK-treated sheath remnants. (**A**) STEM images of cross-sectioned LES- (**left**) and LES/ProtK-treated sheath remnants (**right**) after 14 days incubation in SGP + Fe; (**B**) EDX mapping of LES- (**upper**) and LES/Prot K-treated sheath remnants (**lower**). Note the entire distribution of Fe and O in both sheath remnants, suggesting the presence of Fe oxides. (**C**) Mean (± s.d.) atomic percentage of Fe in LES- and LES/ProK-treated sheath remnants before and after incubation in SGP + Fe. n = 10 spots per sample.

4. Conclusions

In uninoculated SGP + Fe, conversion of Fe(0) to Fe(III) via Fe(II) results in formation of particles that are composed of Fe(III), Si and P and are nearly 50 nm diameter, suggesting that these Fe(III) particles were formed abiotically from components of the SGP medium. The turbidity of SGP + Fe cleared as the population of OUMS1 cells grew. Immediately after whitish primitive sheaths that had been formed separately in SGP were mixed with these Fe(III) particles, the sheaths turned brownish from the attachment of the particles. All these data show that abiotic Fe(III) particles adhered to sheaths of OUMS1. These Fe(III) particles also adhered to the "cell-killed", "cell-lysed", or "LES/ProK-treated" sheaths, indicating that the direct deposition of Fe(III) particles onto the sheath surface was independent of vital activity of cells.

The present study shows only the adherence of Fe(III) particles onto the sheath surface or chemically/enzymatically isolated sheath fibrils, which compose the sheath skeleton, but not the direct adherence onto the surfaces of cells encased with the sheaths. Nevertheless, this phenomenon reminds us of the possibility that this adherence may interfere with the electron generation at the cell surfaces, in particular, at the actively growing region of the sheath terminals [18,22,39].

Our previous work [23] confirmed that Fe(III) is directly deposited on sheaths of strain SP-6 cultured in MSVP amended with various Fe(II) or Fe(III) salts. Considering the present results, we can

reasonably conclude that such a direct deposition of Fe(III) particles onto the sheath surface occurs irrespective of the strain and the medium that contains Fe sources.

The behavior of dissolved metals in natural bodies of water is strongly influenced by particular inorganic and organic materials [40], suggesting that various metal-complexing agents in aquatic systems are involved in complex interactions with microbes and/or their constituent polymers. Thus, microbiologically produced Fe-complexing ligands may play critical roles in both the delivery of Fe(II) to oxidates and the crystallinity of the limited Fe(III) oxyhydroxide observed within the biofilm [41]. As reported in a number of earlier papers [3–6,18,19], an interaction between active groups on bacterial organic components of the sheath skeleton with aqueous-phase inorganics has been considered to hold a key for the metal encrustation of *Leptothrix* sheaths. Although the present data lacks any evidence of an interaction between the net negative surface charge of the sheath material and Fe particles, if the active groups of constituent organics of sheath, even of LES/ProK-treated sheath skeleton fibrils are involved in the disputed adherence of Fe particles onto sheath material, this phenomenon should be adsorption but not simple adherence. Further studies are apparently needed to elucidate the mode of this disputed phenomenon because complicated interactions are expected to occur, more likely between Fe complexes and bacterial organics in sheath materials in component-rich media than in natural hydrosphere. We emphasize that the present results remind us of the necessity to consider that direct adherence of Fe(III) particles onto sheaths may interfere with the mode(s) of sheath encrustation when investigating the interactions between bacterial exopolymers and metal ions, particularly in shake culture using Fe source-containing media.

Acknowledgments: We thank Keiko Toyoda for technical support. We also acknowledge Beth E. Hazen for reviewing and editing the manuscript. This study was financially supported by Japan Science and Technology Agency-Core Research for Evolutional Science and Technology (JST-CREST) (2012–2017) (Jun Takada).

Author Contributions: Tatsuki Kunoh conceived the overall experimental strategy and performed all physiological and microscopic experiments. Hideki Hashimoto and Tomoko Suzuki did the Scanning Transmission Electron Microscopy (STEM), Transmission Electron Microscopy (TEM), and Energy-Dispersive *X*-ray Spectroscopy (EDX) mapping analyses. Naoyuki Hayashi performed the Mössbauer effect analysis. Katsunori Tamura, Mikio Takano, Hitoshi Kunoh, and Jun Takada developed the original concept of the project and/or provided technical advice. All authors participated in writing the manuscript.

Conflicts of Interest: The authors declare no conflict of interest.

References

1. Mann, S. *Biomineralization: Principles and Concepts in Bioinorganic Materials Chemistry*; Oxford University Press: Oxford, UK, 2001.
2. Ghiorse, W.C. Biology of iron- and manganese-depositing bacteria. *Annul. Rev. Microbiol.* **1984**, *38*, 515–550. [CrossRef] [PubMed]
3. Spring, S. The general *Leptothrix* and *Sphaerotilus*. *Prokaryotes* **1979**, *5*, 758–777.
4. Chan, S.C.; Fakra, C.S.; Edwards, C.D.; Emerson, D.; Banfield, F.J. Iron oxyhydroxide mineralization on microbial extracellular polysaccharides. *Geochim. Cosmochim. Acta* **2009**, *73*, 3807–3818. [CrossRef]
5. Ghiorse, W.C.; Hirsch, P. An ultrastructural study of iron and manganese deposition associated with extracellular polymers of pedomicrobium-like budding bacteria. *Arch. Microbiol.* **1979**, *123*, 213–226. [CrossRef]
6. Furutani, M.; Suzuki, T.; Ishihara, H.; Hashimoto, H.; Kunoh, H.; Takada, J. Initial assemblage of bacterial saccharic fibrils and element deposition to form an immature sheath in cultured *Leptothrix* sp. strain OUMS1. *Minerals* **2011**, *1*, 157–166. [CrossRef]
7. Ishihara, H.; Suzuki, T.; Hashimoto, H.; Kunoh, H.; Takada, J. Initial parallel arrangement of extracellular fibrils holds a key for sheath frame construction by *Leptothrix* sp. strain OUMS1. *Minerals* **2013**, *3*, 73–81. [CrossRef]
8. Corstjens, P.L.; de Vrind, J.P.; Westbroek, P.; de Vrind-de Jong, E.W. Enzymatic iron oxidation by *Leptothrix discophora*: Identification of an iron-oxidizing protein. *Appl. Environ. Microbiol.* **1992**, *58*, 450–454. [PubMed]

9. De Vrind-de Jong, E.W.; Corstjens, P.L.; Kempers, E.S.; Westbroek, P.; de Vrind, J.P. Oxidation of manganese and iron by *Leptothrix discophora*: Use of *N*,*N*,*N*′,*N*′-tetramethyl-*p*-phenylenediamine as an indicator of metal oxidation. *Appl. Environ. Microbiol.* **1990**, *56*, 3458–3462. [PubMed]
10. Van Veen, W.L.; Mudler, E.G.; Deinema, M.H. The *Sphaerotilus-Leptothrix* group of bacteria. *Microbiol. Rev.* **1978**, *42*, 329–356. [PubMed]
11. Adams, L.F.; Ghiorse, W.C. Physiology and ultrastructure of *Leptothrix discophora* SS-1. *Arch. Microbiol.* **1986**, *145*, 126–135. [CrossRef]
12. Chan, C.S.; de Stasio, G.; Welch, S.A.; Girasole, M.; Frazer, B.H.; Nesterova, M.V.; Fakra, S.; Banfield, J.F. Microbial polysaccharides template assembly of nanocyrstal fibers. *Science* **2004**, *303*, 1656–1658. [CrossRef] [PubMed]
13. Rentz, J.A.; Kraiya, C.; Luther, G.W., III; Emerson, D. Control of ferrous iron oxidation within circumneutral microbial iron mats by cellular activity and autocatalysis. *Environ. Sci. Technol.* **2007**, *41*, 6084–6089. [CrossRef] [PubMed]
14. Adams, L.F.; Ghiorse, W.C. Characterization of extracellular Mn^{2+}-oxidizing activity and isolation of an Mn^{2+}-oxidizing protein from *Leptothrix discophora* SS-1. *J. Bacteriol.* **1987**, *169*, 1279–1285. [PubMed]
15. Boogerd, F.C.; de Vrind, J.P. Manganese oxidation by *Leptothrix discophora*. *J. Bacteriol.* **1987**, *169*, 489–494. [PubMed]
16. Adams, L.F.; Ghiorse, W.C. Oxidation state of Mn in the Mn oxide produced by *Leptothrix discophora* SS-1. *Geochim. Cosmochim. Acta* **1988**, *52*, 2073–2076. [CrossRef]
17. Emerson, D.; Ghiorse, W.C. Isolation, cultural maintenance, and taxonomy of a sheath-forming strain of *Leptothrix discophora* and characterization of manganese-oxidizing activity associated with the sheath. *Appl. Environ. Microbiol.* **1992**, *58*, 4001–4010. [PubMed]
18. Takeda, M.; Makita, H.; Ohno, K.; Nakahara, Y.; Koizumi, J. Structural analysis of the sheath of a sheathed bacterium, *Leptothrix cholodnii*. *Int. J. Biol. Macromol.* **2005**, *37*, 92–98. [CrossRef] [PubMed]
19. Emerson, D.; Ghiorse, W.C. Ultrastructure and chemical composition of the sheath of *Leptothrix discophora* SP-6. *J. Bacteriol.* **1993**, *175*, 7808–7818. [PubMed]
20. Suzuki, T.; Hashimoto, H.; Ishihara, H.; Kasai, T.; Kunoh, H.; Takada, J. Structural and spatial associations between Fe, O, and C in the network structure of the *Leptothrix ochracea* sheath surface. *Appl. Environ. Microbiol.* **2011**, *77*, 7873–7875. [CrossRef] [PubMed]
21. Sawayama, M.; Suzuki, T.; Hashimoto, H.; Kasai, T.; Furutani, M.; Miyata, N.; Kunoh, H.; Takada, J. Isolation of a *Leptothrix* strain, OUMS1, from ocherous deposits in groundwater. *Curr. Microbiol.* **2011**, *63*, 173–180. [CrossRef] [PubMed]
22. Emerson, D.; Fleming, E.J.; McBeth, J.M. Iron-oxidizing bacteria: An environmental and genomic perspective. *Annu. Rev. Microbiol.* **2010**, *64*, 561–583. [CrossRef] [PubMed]
23. Kunoh, T.; Hashimoto, H.; McFarlane, R.I.; Hayashi, N.; Suzuki, T.; Taketa, E.; Tamura, K.; Takano, M.; El-Naggar, Y.M.; Kunoh, H.; *et al*. Abiotic deposition of Fe complexes onto *Leptothrix* sheaths. *SpringerPlus* **2016**. under review.
24. Hashimoto, H.; Kobayashi, G.; Sakuma, R.; Fujii, T.; Hayashi, N.; Suzuki, T.; Kanno, R.; Takano, M.; Takada, J. Bacterial nanometric amorphous Fe-based oxide: A potential lithium-ion battery anode material. *ACS Appl. Mater. Interfaces* **2014**, *6*, 5374–5378. [CrossRef] [PubMed]
25. Sakuma, R.; Hashimoto, H.; Kobayashi, G.; Fujii, T.; Nakanishi, M.; Kanno, R.; Takano, M.; Takada, J. High-rate performance of a bacterial iron-oxide electrode material for lithium-ion battery. *Mater. Lett.* **2015**, *139*, 414–417. [CrossRef]
26. Ema, T.; Miyazaki, Y.; Kozuki, I.; Sakai, T.; Hashimoto, H.; Takada, J. Highly active lipase immobilized on biogenous iron oxide via an organic bridging group: The dramatic effect of the immobilization support on enzymatic function. *Green Chem.* **2011**, *13*, 3187–3195. [CrossRef]
27. Ema, T.; Miyazaki, Y.; Taniguchi, T.; Takada, J. Robust porphyrin catalysts immobilized on biogenous iron oxide for the repetitive conversions of epoxides and CO_2 into cyclic carbonates. *Green Chem.* **2013**, *15*, 2485–2492. [CrossRef]
28. Mandai, K.; Korenaga, T.; Ema, T.; Sakai, T.; Furutani, M.; Hashimoto, H.; Takada, J. Biogenous iron oxide-immobilized palladium catalyst for the solvent-free Suzuki–Miyaura coupling reaction. *Tetrahedron Lett.* **2012**, *53*, 329–332. [CrossRef]

29. Hashimoto, H.; Asaoka, H.; Nakano, T.; Kusano, Y.; Ishihara, H.; Ikeda, Y.; Nakanishi, M.; Fujii, T.; Yokoyama, T.; Horiishi, N.; *et al*. Preparation, microstructure, and color tone of microtubule material composed of hematite/amorphous-silicate nonocomposite from iron oxide of bacterial origin. *Dye. Pigment*. **2012**, *95*, 639–643.
30. Ishihara, H.; Hashimoto, H.; Taketa, E.; Suzuki, T.; Mandai, K.; Kunoh, H.; Takada, J. Silicon-rich, iron oxide microtubular sheath produced by an iron-oxidizing bacterium, *Leptothrix* sp. strain OUMS1, in culture. *Minerals* **2014**, *4*, 565–577.
31. Suzuki, T.; Kunoh, T.; Nakatsuka, D.; Hashimoto, H.; Tamura, K.; Kunoh, H.; Takada, J. Use of iron powder to obtain high yields of *Leptothrix* sheaths in culture. *Minerals* **2015**, *5*, 335–345. [CrossRef]
32. Luman, C.R.; Castellano, F. *Comprehensive Coordination Chemistry II*; McCleverty, J.A., Meyer, T.J., Eds.; Elsevier: Amsterdam, The Netherlands, 2003; pp. 25–39.
33. Hashimoto, H.; Fujii, T.; Nakanishi, M.; Kusano, Y.; Ikeda, Y.; Takada, J. Synthesis and magnetic properties of magnetite-silicate nanocomposites derived from iron oxide of bacterial origin. *Mater. Chem. Phys.* **2012**, *136*, 1156–1161. [CrossRef]
34. Singer, P.C.; Stumm, W. Acidic mine drainage: The rate-determining step. *Science* **1970**, *167*, 1121–1123. [CrossRef] [PubMed]
35. Emerson, D.; Garen, E.R.; Ghiorse, C.W. Formation of metallogenium-like structures by a manganese-oxiding fungus. *Arch. Microbiol.* **1989**, *151*, 223–231. [CrossRef]
36. Vollrath, S.; Behrends, T.; Koch, C.B.; van Cappellen, P. Effects of temperature on rates and mineral products of microbial Fe(II) oxidation by *Leptothrix cholodnii* at microaerobic conditions. *Geochim. Cosmochim. Acta* **2013**, *108*, 107–124. [CrossRef]
37. Vollrath, S.; Behrends, T.; van Cappellen, P. Oxygen dependency of neutorphilic Fe(III) oxidation by *Leptothrix* differs from abiotic reaction. *Geomicrobiol. J.* **2012**, *29*, 550–560. [CrossRef]
38. Takeda, M.; Kondo, K.; Yamada, M.; Koizumi, J.; Mashima, T.; Matsugami, A.; Katahira, M. Solubilization and structural determination of a glycoconjugate which is assembled into the sheath of *Leptothrix cholodnii*. *Int. J. Biol. Macromol.* **2010**, *46*, 206–211. [CrossRef] [PubMed]
39. Fleming, E.J.; Langdon, A.E.; Martinez-Garcia, M.; Stepanauskas, R.; Poulton, N.J.; Masland, E.D.; Emerson, D. What's new is old: Resolving the identity of *Leptothrix ochracea* using single cell genomics, pyrosequencing and fish. *PLoS ONE* **2011**, *6*. [CrossRef] [PubMed]
40. Ferris, F.G.; Schultze, S.; Witten, T.C.; Fyfe, W.S.; Beveridge, T.J. Metal interactions with microbial biofilms in acidic and neutral pH environments. *Appl. Environ. Microbiol.* **1989**, *55*, 1249–1257. [PubMed]
41. Toner, B.M.; Santelli, C.M.; Marcus, M.A.; Wirth, R.; Chan, C.S.; McCollom, T.; Bach, W.; Edwards, J.K. Biogenic iron oxyhydroxide formation at mid-ocean ridge hydrothermal vents: Juan de Fuca Ridge. *Geochim. Cosmochim. Acta* **2009**, *73*, 388–403. [CrossRef]